Integrated Detection and Tracking via Closed-Loop Radar with Spatial-Domain Matched Illumination

Pete Nielsen[1] and Nathan A. Goodman[2]

Department of Electrical and Computer Engineering, The University of Arizona
1230 E. Speedway Blvd, Tucson, Arizona 85721 USA
[1]pnielsen@email.arizona.edu
[2]goodman@ece.arizona.edu

***Abstract*— We develop a framework for closed-loop detection and tracking of targets. The framework is based on a Bayesian representation that assigns probabilities to potential realizations of the radar channel. In this case, different realizations are characterized by different number and locations of targets present. The Bayesian channel representation can then be used to customize a transmit illumination pattern. The probabilistic representation is updated based on received measurements and Kalman-based prediction of the states of possible targets. Simulation results from a trial experiment of the closed-loop system are provided.**

I. INTRODUCTION

Adaptive and knowledge-based (KB) signal processing focus on improving radar performance through advanced signal processing at the receive end of the system. However, rather than develop transmission waveforms and signal-processing techniques independently, it is useful to consider the implementation and performance of closed-loop radar systems that possess an adaptive radar transmitter that reacts dynamically to the propagation environment and to previously received data. This type of system, termed cognitive radar in [1] or an active-testing system in [2-5], is based on a probabilistic representation of the possible realizations of the radar propagation channel. Rather than operate based on a predefined pattern for search, acquisition, and track, the adaptive transmitter of a cognitive radar system continually interrogates the environment in order to reduce uncertainty associated with the different channel hypotheses. Thus, the probabilistic model guides the system's active interrogations.

In [6], we presented a closed-loop framework for radar target identification. The essential components of the framework included 1) an ensemble of possible propagation channels (in [6], the ensemble was comprised of a set of known target impulse responses); 2) a probabilistic rating assigned to each alternative in the ensemble; 3) waveform design strategies for detecting the true hypothesis as efficiently as possible; 4) a Bayesian update to the probabilities with each data collection; and 5) a termination criterion. In [6], we used sequential hypothesis testing to determine when to terminate the experiment, and two different matched waveform techniques were compared. The first waveform technique was an extension of waveform design based on mutual information [7]. The second technique was based on SNR considerations as suggested in [8-9].

In this paper, we consider spatial-domain application of the mutual-information-based matched waveform technique in order to develop and test a closed-loop implementation of target detection and tracking. Through the equivalence of angle of arrival with spatial frequency, we develop a probabilistic representation of potential target locations in $\left(k_x, k_y, \omega_D\right)$ space. This probabilistic representation can then be converted into a two-dimensional *spectral variance function* (k_x and k_y) upon which the waterfilling [7] operation can be applied to find a matched transmit beampattern. However, since the target model includes Doppler shift (ω_D), potential targets can move between the time when the ensemble is updated with a data collection and the time in the future when the next transmission will occur. Thus, we also use a Kalman-based prediction step to anticipate the status of the probabilistic channel representation at the time when the transmission will occur. The result is a system that performs fully integrated search and track functions. Furthermore, the system scans and shapes its transmit beam not according to a pre-defined or fixed timeline, but according to the uncertainty of the probabilistic model.

The radar signal model is described in Section II, the spatial domain matched illumination strategy is described in Section III, and other details necessary for closed-loop operation are described in Section IV. Simulated results are presented in Section V, and we make our conclusions in Section VI.

II. SIGNAL MODEL

Our goal in this paper is to demonstrate concepts of closed-loop radar such as adaptive illumination based on probabilistic channel representation. Therefore, we employ a simplified signal model that ignores range resolution, ground clutter, and jamming. As far as range resolution, one can assume that the radar system transmits a very narrowband or continuous-wave signal. We make this assumption on the signal model in order to be clear that we are performing spatial-domain spectral shaping, not temporal waveform shaping. Temporal waveform shaping was the subject of [6], and joint spatio-temporal waveform shaping will be the subject of future work.

Let a radar system illuminate a radar channel with a narrowband signal. The geometry, which is depicted in Fig. 1, is similar to a look-down geometry for detecting moving targets on the Earth's surface except for the aforementioned assumption on ground clutter. The primary axes for the system's antenna array elements are the *x*- and *y*-directions.

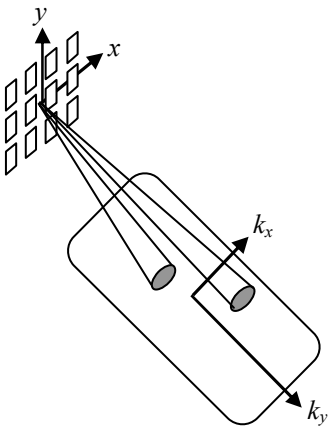

Figure 1. Geometry of the radar signal model.

Element position in the *x*-direction produces a measured phase shift dependent on spatial frequency component k_x. Element position in the *y*-direction enables measurement of the k_y spatial frequency component. In a look-down geometry, k_x and k_y would be related to azimuth and elevation angles, respectively. Moreover, look-down geometries are often defined such that elevation angle uniquely defines target range. Although our system has no range resolution, the relationship between k_y and target range implies that Doppler (range rate) measurements can be related to k_y rate, or $\dot{k}_y$. Using a far-field approximation, the relationship between $\dot{k}_y$ and target Doppler is a constant. Hence, defining positive Doppler shift to mean relative motion toward the radar system, we have

$$\omega_D = -\beta \dot{k}_y \tag{1}$$

where β is a positive constant.

On transmit, the antenna elements act as a phased-array in order to shape the transmit beam. Let the two-dimensional (voltage) pattern of the transmit beam be denoted by $S\left(k_x, k_y\right)$. Note that use of a capital '*S*' as well as k_x and k_y emphasize that the transmit beam pattern is a spatial-frequency-domain representation of the transmit waveform. In other words, $S\left(k_x, k_y\right)$ can be found from a two-dimensional discrete-time Fourier Transform of the amplitude and phase of each antenna element. On receive, the antenna array acts as a multi-channel system such that the output of each antenna element is measured.

Let the q^{th} target existing within the illumination pattern of the radar be characterized by a complex reflection coefficient α_q, spatial frequency coordinates $k_x^{(q)}$ and $k_y^{(q)}$, and a Doppler shift $\omega_D^{(q)}$. Hence, the received signal at the $(m,n)^{\text{th}}$ antenna and p^{th} time sample due to the q^{th} target is

$$v\left(m,n,p\right) = S\left(k_x^{(q)}, k_y^{(q)}\right)\alpha_q \exp\left(-j\left(k_x^{(q)} x_m + k_y^{(q)} y_n - \omega_D^{(q)} t_p\right)\right). \tag{2}$$

Data samples are collected over *M* antennas in the *x*-direction and *N* antennas in the *y*-direction for a total of *MN* spatial measurements. Samples are also collected at *P* time instants, and the relative phase of all *MNP* measurements are stacked into a space-time steering vector $\mathbf{a}\left(k_x, k_y, \omega_D\right)$. The total received signal vector is then

$$\mathbf{v} = S\left(k_x^{(q)}, k_y^{(q)}\right)\alpha_q \mathbf{a}\left(k_x^{(q)}, k_y^{(q)}, \omega_D^{(q)}\right). \tag{3}$$

Next, allowing for *Q* targets, the measurement vector due to all targets for a single transmission is

$$\mathbf{z} = \sum_{q=1}^{Q} S\left(k_x^{(q)}, k_y^{(q)}\right)\alpha_q \mathbf{a}\left(k_x^{(q)}, k_y^{(q)}, \omega_D^{(q)}\right) + \mathbf{w} \tag{4}$$

where $\mathbf{w}$ is a vector of additive white Gaussian noise.

The measurement model in (2) clearly indicates that the signal reflected from a target and incident on the system is a three-dimensional sinusoid with frequencies $\left(k_x^{(q)}, k_y^{(q)}, \omega_D^{(q)}\right)$. Therefore, a frequency-domain representation of the signal component is

$$V\left(k_x, k_y, \omega_D\right) = S\left(k_x, k_y\right) H\left(k_x, k_y, \omega_D\right) \tag{5}$$

where

$$H\left(k_x, k_y, \omega_D\right) = \sum_{q=1}^{Q} \alpha_q \delta\left(k_x - k_x^{(q)}, k_y - k_y^{(q)}, \omega_D - \omega_D^{(q)}\right) \tag{6}$$

and $\delta\left(k_x, k_y, \omega_D\right)$ is a three-dimensional delta function. The data-domain space-time data are then obtained by the transformation

$$\mathbf{z} = \iiint_{k_x, k_y, \omega_D} V\left(k_x, k_y, \omega_D\right)\mathbf{a}\left(k_x, k_y, \omega_D\right) dk_x dk_y d\omega_D + \mathbf{w}, \tag{7}$$

which by substitution of (5) and (6) and application of the sifting property becomes (4). The function $H\left(k_x, k_y, \omega_D\right)$ is the transfer function of the radar channel, which will be used in the next section to help define the adaptive transmit beampattern.

From (4) we see that the transmit pattern significantly affects the received signal. In particular, the transmit pattern controls the SNR of any signals reflected from targets, which in turn affects the system's ability to detect the target and estimate its parameters. For the closed-loop radar paradigm, SNR affects the system's ability to update the probabilistic ratings of the different channel alternatives. For the application described in this paper, different channel alternatives consist of different combinations of the number and location of targets in $\left(k_x, k_y, \omega_D\right)$ space.

III. Spatial-Domain Matched Illumination

In this section, we summarize the information-based matched illumination technique of [7] and then describe how we apply the technique to the design of transmit beamforming for closed-loop radar.

Let $\mathbf{h}\left(t\right)$ be a random process that can be thought of as an ensemble of impulse responses. We will assume that all of the sample functions of $\mathbf{h}\left(t\right)$ have finite energy and are causal

impulse responses. If we further assume that $\mathbf{h}(t)$ is a Gaussian random process, then we can find the waveform that maximizes the mutual information between the ensemble of impulse responses and the received waveform. Let the waveform have finite energy E, be confined to the time interval $-T/2 < t < T/2$, and be essentially bandlimited such that most of its energy is contained within the frequency band $|f| \le 1/2T_s$. The information-maximizing waveform under these constraints has the magnitude-squared spectrum defined by [7]

$$|S(f)|^2 = \begin{cases} \max\left[0, A - \dfrac{\sigma_n^2 T_y}{2\sigma_H^2(f)}\right] & |f| \le \dfrac{1}{2T_s} \\ 0 & |f| > \dfrac{1}{2T_s} \end{cases} \quad (8)$$

where T_y is the interval during which the received signal is observed and the quantity $\sigma_H^2(f)$ is called the spectral variance and is defined by

$$\sigma_H^2(f) = \mathrm{E}\left\{\left|\mathbf{H}(f) - \mathrm{E}\{\mathbf{H}(f)\}\right|^2\right\}. \quad (9)$$

The spectral variance function quantifies the uncertainty in the ensemble of target transfer functions at frequency f. The constant A in (8) enforces the finite-energy constraint by solving

$$E = \int_{-1/2T_s}^{1/2T_s} \max\left[0, A - \frac{\sigma_n^2 T_y}{2\sigma_H^2(f)}\right] df \,. \quad (10)$$

The solution in (8) is obtained by performing the waterfilling action [7] on the function $\sigma_n^2 T_y / 2\sigma_H^2(f)$. In [6], we integrated matched illumination techniques with sequential hypothesis testing in order to efficiently determine the true impulse from among a finite number of known alternatives. Although the ensemble in [6] was not Gaussian, we computed a spectral variance according to

$$\sigma_H^2(f) = \sum_{m=1}^{M} P_m |H_m(f)|^2 - \left|\sum_{m=1}^{M} P_m H_m(f)\right|^2 \quad (11)$$

where P_m and $H_m(f)$ were, respectively, the probability and transfer function associated with the m^{th} hypothesis. It was found in [6] that waterfilling on the spectral variance function in (11) produced waveforms that performed very well in that application.

Hence, in this paper, we propose to compute spatial illumination functions, also known as the transmit beampattern, by waterfilling on a spatial-spectral variance function, $\sigma_H^2(k_x, k_y)$. This function can be obtained in a similar manner as (11) by using the channel transfer function defined by (6) for various channel hypotheses. Each time an observation is made, the probability function describing the likelihood of the different hypotheses is updated, which results in a new spatial-spectral variance function and new transmit beampattern for the next observation.

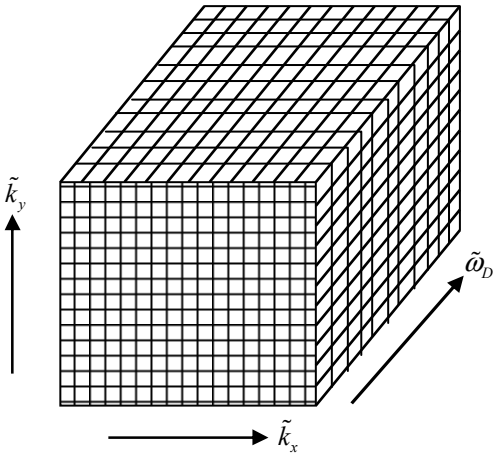

Figure 2. Discrete target parameter (hypothesis) space.

Before this spatial-domain waterfilling can occur, however, some additional details must be addressed. First, in this application there truly are an infinite number of hypotheses. Since the target parameters are continuous, there are an infinite number of values they can take – even if they are limited to within a finite range. Furthermore, there are also many permutations of the radar channel that depend on the number of targets present. In order to compute a spectral variance in the style of (11), the number of hypotheses must be limited to a reasonable number. Second, the transfer function defined in Section II above is a three-dimensional function of k_x, k_y, and ω_D, yet a spatial-only illumination pattern can only control illumination in the k_x and k_y dimensions, not the ω_D dimension. Hence, a three-dimensional channel transfer function with an infinite number of possible realizations must be reduced to a two-dimensional spectral variance function with a manageable number of possible realizations.

First, we propose to reduce the number of hypotheses by dividing the three-dimensional target parameter space into a three-dimensional hypothesis grid. Let the normalized target parameters $\tilde{k}_x$, $\tilde{k}_y$, and $\tilde{\omega}_D$ each be confined to the interval $[-\pi, \pi]$ and let the parameter volume be divided into cells as depicted in Fig. 2. For the moment, the dimensions of the cells are determined by maximum system resolution, which is controlled by the size of the antenna array and the time duration, T, of a single observation interval. Each cell in the volume represents a different combination of target location (k_x and k_y) and Doppler shift. Furthermore, each cell is assigned a probability that quantifies the current system understanding of whether or not a target is present in that cell.

Unfortunately, even for a simplified, low-resolution system with, say, 10 cells in each dimension, there are $10^3 = 1000$ cells that may or may not possess a target. The number of

channel hypotheses is even larger, but the problem can be simplified by noting that the spectral variance of each (k_x,k_y) cell can be calculated separately from the others. In other words, for a given (k_x,k_y) cell, we only need to consider the different hypotheses along the Doppler dimension. Furthermore, we propose to treat the decision of target presence in the individual cells of the target volume as independent. With this assumption, the total variance in a (k_x,k_y) cell is the sum of the variances in the different Doppler bins of that cell.

Consider the i^{th} Doppler bin for a particular (k_x,k_y) cell in the volume of Fig. 2, and let the current probability of target presence in that cell be $P\left(i;k_x,k_y\right)$. Suppose that if a target is present in that bin, that its reflection coefficient is α_i. According to (6), if the target is present, the transfer function value for that cell is equal to the target's reflection coefficient. There are two hypotheses for that cell – a target is either present or not. Substituting these two hypotheses into the "finite-hypothesis" spectral variance calculation of (11), the variance for that cell becomes

$$\begin{aligned}\sigma^2 &= \left[P\left(i;k_x,k_y\right)\left|\alpha_i\right|^2 + \left(1-P\left(i;k_x,k_y\right)\right)\left(0\right)^2 \right] \\ &\quad - \left| P\left(i;k_x,k_y\right)\alpha_i + \left(1-P\left(i;k_x,k_y\right)\right)\left(0\right) \right|^2 . \\ &= P\left(i;k_x,k_y\right)\left|\alpha_i\right|^2 - P\left(i;k_x,k_y\right)^2\left|\alpha_i\right|^2\end{aligned} \quad (12)$$

Then, under the assumption that the decisions in different cells are independent, the total variance for a particular (k_x,k_y) bin is

$$\sigma^2\left(k_x,k_y\right) = \sum_{i=1}^{N_D} P\left(i;k_x,k_y\right)\left|\alpha_i\right|^2 - P\left(i;k_x,k_y\right)^2\left|\alpha_i\right|^2 \quad (13)$$

where N_D is the number of cells in the Doppler dimension.

Our proposed system applies the spectral variance calculation of (13) to each (k_x,k_y) bin and then performs the waterfilling operation of the spectral variance function to determine the adaptive transmit power pattern for the next illumination.

IV. Additional Closed-Loop Details

In the previous sections, we have described our radar signal model and the proposed technique for matching the transmit illumination pattern to the probabilistic representation of the radar channel. We have taken the mutual-information-based matched waveform of [7] and adapted it to our scenario where our hypotheses do not form a Gaussian ensemble. However, two requirements of our cognitive radar system have not yet been addressed. First, we have not described how to update the probabilities associated with the cells in the target volume. Second, the fact that the target is allowed to possess Doppler shift implies that the target is moving. In the following sub-sections, we deal with these two issues and then summarize the system.

A. Bayesian Probability Updates

To update the probabilities associated with each target cell, we apply Bayes' rule. Let $\mathbf{z}_i$ be the space-time data observed due to the radar system's i^{th} transmission, and H_0 and H_1 be the null and target-present hypotheses of a particular target cell. According to Bayes' rule, the probability that a target is present in a given cell after observation of $\mathbf{z}_i$ is

$$P\left(H_1 \mid \mathbf{z}_i\right) = \frac{P\left(\mathbf{z}_i \mid H_1\right)P\left(H_1 \mid \mathbf{z}_{i-1}\right)}{p\left(\mathbf{z}_i\right)} \quad (14)$$

where the lowercase 'p' denotes a probability density function. The probability that a target is not present is

$$P\left(H_0 \mid \mathbf{z}_i\right) = \frac{P\left(\mathbf{z}_i \mid H_0\right)P\left(H_0 \mid \mathbf{z}_{i-1}\right)}{p\left(\mathbf{z}_i\right)} . \quad (15)$$

The denominator in (14) and (15) is difficult, if not impossible, to evaluate. However, since the denominator is the same for both hypotheses, it essentially serves as a scaling factor such that the sum of the two probabilities is unity. In practice, rather than evaluate the denominator, we instead evaluate the numerator in (14) and (15), then scale the results for a total probability of one.

One nice feature of the Bayesian probability update is that the current probability depends on the previous probability, which in turn depends on the probability before that, and so on. Hence, all that has been learned by the system from prior measurements is retained in the recursive probability calculation, even if the measurements themselves are not stored. This feature of state-space models is noted in [1].

B. Probability Prediction Due to Target Motion

The second requirement that still needs to be addressed is how to deal with targets in motion. Doppler-shifted targets implies that target motion is present, and our signal model specifically relates Doppler shift to the target's rate of change in k_y. After measuring $\mathbf{z}_i$, the system updates the probability in each hypothesis cell according to (14) and (15). However, if the target is moving, it may have moved into a different cell by the time the transmission occurs. This causes the probabilities updated with measurement $\mathbf{z}_i$ to be out of date by the time the $(i+1)^{\text{th}}$ transmission occurs. Therefore, the probabilities must be propagated forward in time to the point when the next transmission will occur.

Changing target parameters and Bayesian channel representation suggest the relevance of a Kalman filter-based approach. We use the Kalman prediction equations to update the target parameter state and covariance, which can then be used to determine the probability that the target will be within a particular target parameter cell at some time in the future.

First, it would be inefficient to propagate the probability in every single target parameter cell. Instead, we perform a soft detection step to narrow the number of possible channel hypotheses to those with a reasonable current probability of having a target present. Any probability update from (14) that

exceeds a certain threshold is declared to be a potential target. We then perform a maximum likelihood search within the associated target parameter cell. This provides a finer estimate of the potential target's true parameters. Suppose the soft detection occurs after the i^{th} observation. The estimates are placed into a state vector according to

$$\mathbf{u}_i = \begin{bmatrix} \hat{k}_x & \hat{k}_y & \hat{\dot{k}}_y \end{bmatrix}^{\mathrm{T}}. \tag{16}$$

Furthermore, we can also initialize the covariance associated with the current target state. Let this covariance matrix be $\mathbf{M}_i$. The linear target motion model results in the predicted target state at the next transmission (ΔT seconds later) according to

$$\mathbf{u}_{i+1} = \mathbf{A}\mathbf{u}_i \tag{17}$$

where

$$\mathbf{A} = \begin{bmatrix} 1 & 0 & 0 \\ 0 & 1 & \Delta T \\ 0 & 0 & 1 \end{bmatrix}. \tag{18}$$

After applying the Kalman prediction equations, the target state is assumed to be a three-dimensional Gaussian random vector with mean $\mathbf{A}\mathbf{u}_i$ and predicted covariance

$$\mathbf{M}_{i+1} = \mathbf{A}\mathbf{M}_i\mathbf{A} + \mathbf{R}_g. \tag{19}$$

where $\mathbf{R}_g$ is the covariance of the input noise process that models target maneuverability. Therefore, the probability that this soft-detected target falls within a particular cell of the target parameter space shown in Fig. 2 is equal to the integral of the pdf of the random state vector over the volume of the cell. Most of the probability will occur in the cell where the target's predicted state vector lies. Other nearby cells will also have some probability that this same target is present, depending on the quality of the parameter estimation and the maneuverability of the target. Also, by (18) we see that the k_x state is not coupled with the other two parameters. Hence, the integration can be broken into a one-dimensional integration for k_x and a two-dimensional integration for k_y and $\dot{k}_y$.

In summary, any target parameter cells that are not illuminated by the transmit beam pattern retain their probabilities for the next spectral variance calculation. Any illuminated cells are updated with the Bayesian equations of (14) and (15). Finally, if after the Bayesian update any cell exceeds a pre-determined threshold for soft detection, the potential target state in that cell is estimated and propagated forward to the next transmission.

C. Closed Loop Summary

Figure 3 summarizes the operation of the closed-loop system for integrated detection and tracking. The scenario

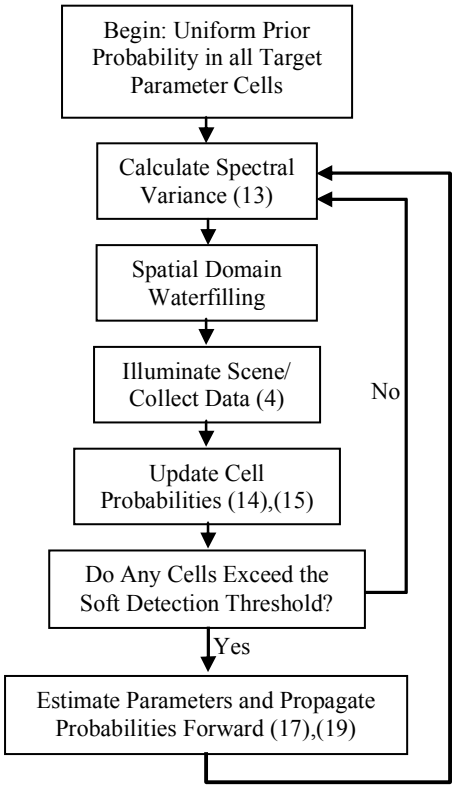

Figure 3. Closed-loop radar flow diagram.

begins with a volume of target parameters cells, each with an initial (low) probability that a target is present. Since the probability distribution is uniform, the first spectral variance and waveform pattern will be flat. From then on, each time data are collected, the cell probabilities are updated and checked for the presence of soft detections. If no soft detections are present, the next spectral variance is calculated based on the probability updates. If a soft detection is obtained, relevant cells are updated by propagating the estimated target state forward to the next transmission time and integrating the predicted pdf.

V. Simulation Results

We now present snapshot results from simulation of the proposed closed-loop system. The parameters for the simulation were as follows. The antenna array was a 10 by 10 rectangular grid, and the number of time samples was also 10. Therefore, the total number of measurements taken in a single illumination was 1000. A single target was added, and the target cell probabilities were all initialized to 0.01.

Figure 4 shows snapshot images of the probability map over spatial frequencies for the zero-Doppler bin where the target was placed, as well as the adaptive illumination pattern. From left to right in Figure 4, each row shows 1) the probabilities in the (k_x,k_y) cells of the target Doppler bin just prior to waterfilling. For all illuminations after the first, this is also the probability map after the possible prediction step; 2) the illumination pattern that results from the probability map in 1); and 3) the probability map after updating with measurements.

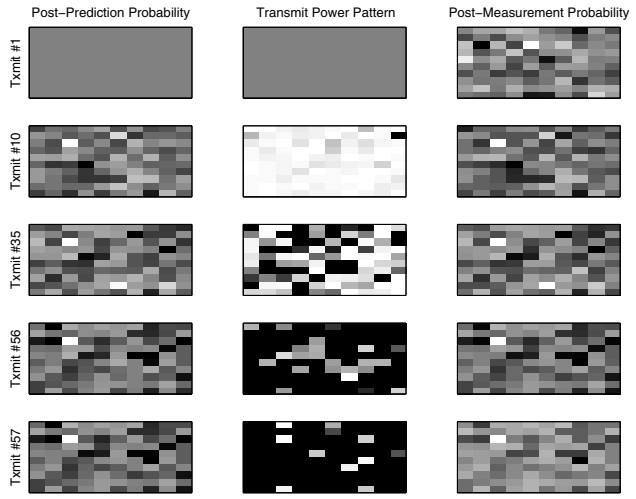

Figure 4. Probability and illumination pattern snapshots at five different illumination times.

One can see that at the first iteration, the probability map prior to illumination is constant, which reflects constant prior probability of target presence. After the first illumination, the probability map for that Doppler bin is no longer constant. At the tenth illumination, the (3,3) cell from the upper left (which is the correct spatial location of the target) is showing some likelihood of target presence, but the illumination pattern is still fairly constant over the spatial bins. At the 35th illumination, the probability of the true target location hasn't changed much from the tenth illumination, but the illumination pattern shows that target presence has been deemed very unlikely in several cells, which is why they receive no illumination power. At the 56th illumination, the (3,3) cell is strong enough to be declared a target. In fact, the target parameters have been measured well enough and the target maneuverability is low enough that the system does not need to put power on the target cell. Instead, power is distributed to other cells where target presence is most likely. In absolute terms, target presence in these cells is unlikely, but relative to other cells and the target track, these cells that receive power in the 56th illumination are the most uncertain. Finally, in the 57th illumination, the target track covariance has widened enough that the system needs to put power on the target to update it again. Although not shown, the system continues to alternate naturally between illuminating and not illuminating the target cell.

VI. Conclusions

We have described a framework for a closed-loop, cognitive radar system that adapts its transmit beam in order to detect and track targets according to a probabilistic representation of the radar channel rather than a fixed pattern of interleaved search and track sweeps. Several steps are required, but the end result is a system that compromises between searching for new targets and updating existing target tracks. The compromise at any given time depends on the radar system's current state of understanding of the channel, which in turn depends on the results from prior illuminations.

References

[1] S. Haykin, "Cognitive radar: a way of the future," *IEEE Sig. Proc. Mag.*, vol. 23, no. 1, pp. 30-40, Jan. 2006.

[2] D.R. Fuhrmann, "Active-testing surveillance systems, or, playing twenty questions with a radar," in *Proc. 11th Annual Adaptive Sensor and Array Processing (ASAP) Workshop*, MIT Lincoln Laboratory, Lexington, MA, Mar. 11-13, 2003 [Cd-Rom]

[3] D.R. Fuhrmann, "Active-testing surveillance for multiple target detection with composite hypotheses," in Proc. 2003 IEEE Workshop on Statistical Signal Proc., pp. 641-644, Oct. 2003.

[4] D.R. Fuhrmann, "One-step optimal measurement selection for linear Gaussian estimation problems," in Proc. 2007 Waveform Diversity and Design Conf., pp. 224-227, June 2007.

[5] D.R. Fuhrmann and G. San Antonio, "Kalman filter and extended Kalman filter using one-step optimal measurement selection," in Proc. 2007 Waveform Diversity and Design Conf., pp. 312-315, June 2007.

[6] N.A. Goodman, P.R. Venkata, and M.A. Neifeld, "Adaptive waveform design and sequential hypothesis testing for target recognition with active sensors," *IEEE J. Sel. Topics in Sig. Proc*, vol. 1, no. 1, pp. 105-113, June 2007.

[7] M.R. Bell, "Information theory and radar waveform design," *IEEE Trans. Info. Theory*, vol. 39, no. 5, pp. 1578-1579, Sept. 1993.

[8] J.R. Guerci and S. U. Pillai, "Theory and Application of Optimum Transmit-Receive Radar," *IEEE 2000 International Radar Conference*, Washington, DC, pp. 705-710, May 8-12, 2000.

[9] D.A. Garren, M.K. Osborn, A.C. Odom, J.S. Goldstein, S.U. Pillai, and J.R. Guerci, "Enhanced target detection and identification via optimised radar transmission pulse shape," *IEEE Proc. Radar, Sonar and Navigation*, 148(3), pp. 130-138, June 2001.